Structural and compositional variations in $ZnSnP_2$/GaAs superlattices

B. Lita, M. Beck, and R. S. Goldman[a)]
Department of Materials Science and Engineering, University of Michigan, Ann Arbor, Michigan 48109

G. A. Seryogin, S. A. Nikishin, and H. Temkin
Department of Electrical Engineering, Texas Tech University, Lubbock, Texas 79409

(Received 28 June 2000; accepted for publication 29 August 2000)

We have investigated the structural and compositional uniformity of a set of $ZnSnP_2$/GaAs superlattices grown by gas-source molecular-beam epitaxy. Cross-sectional scanning tunneling microscopy reveals an asymmetry in interface abruptness, with the $ZnSnP_2$ on GaAs interfaces apparently much smoother than the GaAs on $ZnSnP_2$ interfaces. The increased roughness of the GaAs on $ZnSnP_2$ interface occurs simultaneously with the apparent surface segregation of Sn. High-resolution x-ray diffraction and photoluminescence spectroscopy suggest that the $ZnSnP_2$ regions consist of a mixture of $ZnSnP_2$ and $ZnSnAs_2$. This is further confirmed by cross-sectional scanning tunneling microscopy and spectroscopy, which reveal the presence of nanometer-scale $ZnSnP_2$ and $ZnSnAs_2$-rich regions. Interestingly, these lateral compositional variations are not correlated with observed growth front undulations. © *2000 American Institute of Physics.* [S0003-6951(00)05043-9]

Due to its tetragonal unit cell and direct band gap in the near infrared, $ZnSnP_2$ is promising for a variety of applications including nonlinear optical devices[1] and solar cells.[2] Both ordered (chalcopyrite) and disordered (sphalerite) phases of $ZnSnP_2$ have been grown in bulk form[3] and by liquid phase epitaxy[4,5] with band gaps ranging from 1.25 to 1.64 eV, as the ordering of Zn and Sn on one of the face-centered cubic sublattices is increased.[3] Using epitaxial growth techniques, both ordered and disordered phases of $ZnSnP_2$ may be grown nearly lattice matched to GaAs, providing a means for producing essentially strain-free structures with a variety of band gaps and band offsets.[6,7] A remaining challenge in the preparation of $ZnSnP_2$/GaAs heterostructures is the control of the interface quality and compositional uniformity for a given growth sequence. Therefore, we have investigated the structural, electronic, and optical properties of a set of gas-source molecular beam epitaxially (GSMBE) grown $ZnSnP_2$/GaAs superlattices using ultrahigh vacuum cross-sectional scanning tunneling microscopy (XSTM), scanning tunneling spectroscopy (STS), high-resolution x-ray diffraction (HRXRD), and photoluminescence (PL) spectroscopy. XSTM reveals an asymmetry in interface abruptness, with the $ZnSnP_2$ on GaAs interfaces apparently much smoother than the GaAs on $ZnSnP_2$ interfaces. This asymmetry is likely due to strain-enhanced surface segregation of Sn occurring during the growth of GaAs on $ZnSnP_2$. In the $ZnSnP_2$ regions, STS measurements reveal lateral variations in the effective band gaps. These variations are attributed to the presence of alternating $ZnSnP_2$ and $ZnSnAs_2$ rich regions, which are not correlated with observed growth front undulations. The presence of these compositional variations is further confirmed by HRXRD and PL.

The samples were grown by GSMBE using solid group III sources, and AsH_3 and PH_3 as gas sources. The unintentionally doped heterostructures were grown on epi-ready (001)-oriented n^+ Si-doped GaAs substrates, with a substrate temperature of 350 °C and a Sn/Zn flux ratio of approximately 0.1.[6] The targeted structures included ten-period superlattices capped with 50 nm of GaAs. The superlattices consisted of 20 nm $ZnSnP_2$ quantum wells and 20 nm GaAs barriers.

High-resolution x-ray rocking curves (XRC) were measured with double-axis x-ray diffraction using Cu $K\alpha$ radiation monochromated by a four-reflection monochromator, which employs Si(220) reflections in the $(+, -, -, +)$ configuration. The rocking curves were collected near the GaAs (004) reflection. For XSTM, the samples were cleaved to expose a (110) surface, in a UHV chamber with base pressure $\leqslant 5\times10^{-11}$ Torr.[8] STS measurements were performed using the variable tip-sample separation method.[9] Both STM and STS were performed with electrochemically etched polycrystalline W and commercially available Pt/Ir tips. The tips were cleaned *in situ* by electron bombardment. All images were obtained with a constant tunnel current of 0.09 nA unless specified otherwise, and sample bias voltages listed below.

Figure 1 shows a high-resolution XRC of a superlattice, collected near the GaAs (004) reflection. The presence of satellite peaks up to the third order suggests that the super-

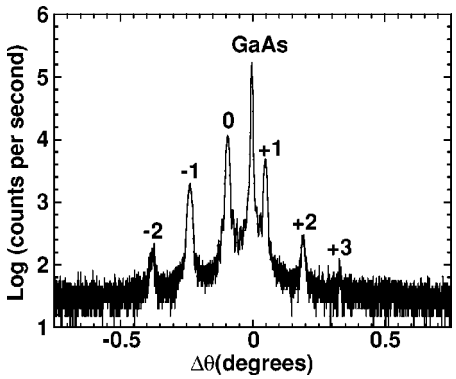

FIG. 1. High-resolution x-ray rocking curve of $ZnSnP_2$/GaAs superlattices collected near the (004) GaAs reflection.

a)Electronic mail: rsgold@engin.umich.edu

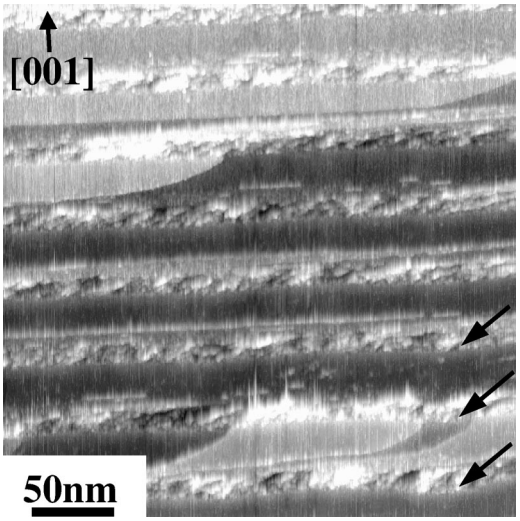

FIG. 2. Large-scale topographic image of superlattices, obtained at a −2.2 V sample bias voltage. The gray-scale range displayed is 19 Å. Undulations of the growth front morphology of the $ZnSnP_2$ on GaAs interfaces are indicated by arrows.

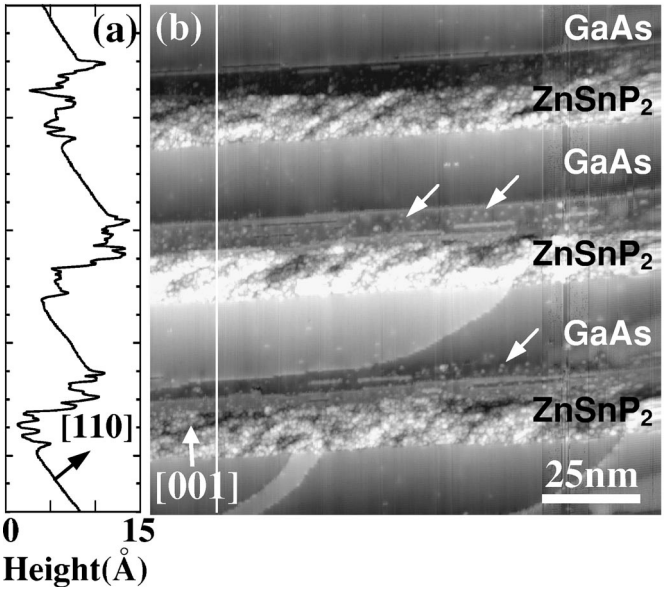

FIG. 3. (b) High-resolution topographic image of superlattices obtained with 0.15 nA tunneling current and −1.8 V sample bias voltage. The gray-scale range displayed is 22 Å. A cut of the tip height along the line indicated in (b) is displayed in (a). Individual atomic-scale defects segregating near the GaAs on $ZnSnP_2$ interfaces are indicated by arrows in (b).

lattices possess a fairly well defined periodic structure. The average spacing between the satellite peaks indicates an average superlattice period of 36.8 ± 0.2 nm. Using the splitting between the GaAs substrate peak and the zero-order reflection of the superlattice, we calculate an average superlattice (004) *d* spacing of 5.667 Å. Interestingly, the (004) *d* spacings of bulk $ZnSnP_2$, in either the ordered (chalcopyrite) or disordered (sphalerite) form, have been reported to be 5.651 ± 0.001 Å,[10] which is *smaller* than that of bulk GaAs (5.5653 Å). Consequently, the average (004) *d* spacing of a superlattice consisting of GaAs and stoichiometric $ZnSnP_2$ *would always be less than that of GaAs*. On the other hand, the (004) *d* spacing of bulk $ZnSnAs_2$ ranges from 5.852[11] to 5.854 Å.[12] Therefore, it is likely that the so-called $ZnSnP_2$ regions actually consist of a mixture of $ZnSnP_2$ and $ZnSnAs_2$. The incorporation of As in the layers is probably due to a chamber memory effect associated with the growth interrupts needed to switch the group V molecular beams.[13]

Figures 2 and 3(b) show XSTM topographic images of the $ZnSnP_2$/GaAs superlattices, displayed with the growth direction from the bottom to the top. In these filled state images, the $ZnSnP_2$ regions appear as inhomogeneous layers sandwiched between homogeneous layers of GaAs. The topographic images in Figs. 2 and 3(b) are displayed at an angle with respect to the normal of the cleaved (110) surface. Hence, the cut of the tip height in Fig. 3(a), defined by the line in Fig. 3(b), reveals a cleaved surface profile which resembles a rotated staircase, with atomically flat GaAs regions surrounding rougher $ZnSnP_2$ regions. Interestingly, the $ZnSnP_2$ on GaAs interfaces are well-defined and nearly atomically abrupt, while the GaAs on $ZnSnP_2$ interfaces are more difficult to discern due to lateral inhomogeneities in the $ZnSnP_2$ region and the presence of a high density of cleavage steps in the vicinity of the interface.

In Fig. 2, lateral variations in the growth surface morphology of the $ZnSnP_2$ on GaAs interfaces are apparent. The amplitude of these growth front undulations decreases gradually towards the top of the structure, essentially disappearing after 3–4 superlattice periods. Similar types of growth front undulations have been observed in other strained-layer superlattice systems.[14] In those cases, the growth front undulations were observed first in a strained layer, and the undulations were attributed to the elastic relaxation of strain. In the $ZnSnP_2$/GaAs system of the present investigation, the growth front undulations originate in the first GaAs layer and therefore may not be driven by elastic relaxation of strain, but rather by generic morphological instabilities occurring during homoepitaxy.

The steps and terraces observed in Fig. 3(b) are apparent in both filled and empty state topographic images (not shown), suggesting that these features are of topographic origin, possibly resulting from the cleaving process. The observed steps are generally oriented parallel to the $ZnSnP_2$/GaAs interfaces, increasing the apparent width of the $ZnSnP_2$ layers. Occasionally, steps located in the vicinity of the GaAs on $ZnSnP_2$ interfaces are aligned up to 45° away from the interface. Similar 45° oriented steps have been observed on the cleaved {110} surfaces of highly mismatched semiconductor heterostructures.[15] Since most of the 45° steps terminate in the $ZnSnP_2$ layers, their formation may be related to significant lateral strains due to the presence of lateral composition fluctuations in these layers. Within the $ZnSnP_2$ layers, alternating protrusions (brighter regions) and depressions (darker regions), spanning tens of nanometers, are apparent. Since these domains appear very similar in filled and empty state images, and the tip height difference between the domains is typically ~1 nm, it is likely that the domain contrast is dominated by topographic effects. In particular, the domain contrast is likely a cleavage-induced surface distortion resulting from the significant lateral strains due to the presence of $ZnSnP_2$- and $ZnSnAs_2$-rich regions. The presence of these lateral compositional fluctuations is supported by the x-ray diffraction data mentioned earlier and STS data which will be discussed below. Interestingly, these

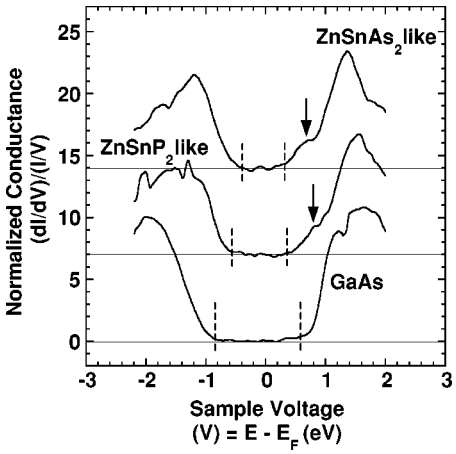

FIG. 4. STS spectra acquired on $ZnSnP_2$ layers, in comparison with a region of clean GaAs. The valence and conduction band edges are marked by vertical dashed lines on the left and right, respectively. A state near the conduction band edge of $ZnSnP_2$ is indicated by downward pointing arrows. The sample voltage corresponds to the energy of the state relative to the Fermi level.

lateral compositional fluctuations do not appear to be correlated with the growth front undulations discussed above.

Circular bright features near the GaAs on $ZnSnP_2$ interfaces are only observed in filled state images, such as that in Fig. 3(b). Since the apparent diameters of these features are generally less than 1 nm, they are mainly attributed to individual atomic-scale defects. Furthermore, since filled state images probe the energy and spatial extent of the dangling bonds of the group V sublattice, these features are likely related to a point defect on the arsenic sublattice. Earlier filled state XSTM studies of arsenide–phosphide heterostructures showed phosphide interlayers which appeared dark in comparison to the surrounding GaAs.[16] Furthermore, earlier work on Zn doping in GaAs showed that the Zn_{Ga} defects appeared bright with respect to the surrounding GaAs, for both empty and filled state images.[17] The corresponding arsenic vacancy appeared dark and bright in filled and empty state images, respectively.[18] Since our point defects appear bright in filled state images and are not observed in empty state images, it is unlikely that these are due to P_{As}, Zn_{Ga}, or V_{As}. Instead, we attribute the point defects to individual Sn atoms, which have been reported to segregate at the surface during the growth of GaAs doped with Sn.[19,20] In addition, a higher density of cleavage-related steps is observed in the proximity of the GaAs on $ZnSnP_2$ interfaces, suggesting a higher residual strain at these interfaces.[21] Hence, the mechanism for the interface asymmetry is likely strain-enhanced surface segregation of Sn during the growth of GaAs on $ZnSnP_2$. Furthermore, as the apparent segregation of Sn occurs near the GaAs on $ZnSnP_2$ interfaces, independent of vertical location with respect to the GaAs substrate, it is unlikely that the segregation of Sn is related to the growth front instabilities discussed earlier.

In Fig. 4, the normalized conductance versus sample bias voltage is plotted for $ZnSnP_2$ regions and compared with regions of clean GaAs. The GaAs spectrum, shown at the bottom of the figure, displays well-defined band edges, with a band gap of 1.43 ± 0.1 eV, comparable to that of bulk GaAs. In the $ZnSnP_2$ regions, 10–20 nm spaced lateral variations in the effective band gaps are observed and may be attributed to alternating regions of disordered $ZnSnP_2$ and $ZnSnAs_2$, whose bulk band gaps are 1.24 and 0.75 eV, respectively. This explanation is further supported by room temperature PL measurements which show a broad peak centered at approximately 1 eV. Our STS measurements also reveal a state near the conduction band edge of $ZnSnP_2$. The energetic position of this state with respect to the Fermi level is similar to that observed in studies of Sn deposition on GaAs surfaces,[22] suggesting that it is a Sn-induced state. Whether this state is a Sn-induced surface state or a state characteristic of bulk $ZnSnP_2$ remains to be determined.

Based upon our observations of lateral composition variations and an earlier report on the average lattice constant dependence on the Sn/Zn flux ratio,[6] we suggest that the incorporation of As in the $ZnSnP_2$ layers may be minimized by a further increase in the Sn/Zn flux ratio. Further work is currently in progress to determine the dependence of the Sn/Zn flux ratio and additional growth parameters on the compositional uniformity of $ZnSnP_2$/GaAs superlattices.

The work at University of Michigan was supported in part by the donors of the Petroleum Research Fund, administered by the American Chemical Society, and the National Science Foundation Research Experiences for Undergraduates Program. The work at Texas Tech University was supported by the J. F. Maddox Foundation. The authors also thank R. M. Feenstra for sharing his code for scanning tunneling spectroscopy analysis.

[1] M. C. Ohmer and R. Pandey, MRS Bull. **23**, 16 (1998), and references therein.
[2] E. A. Patten, G. A. Davis, S. J. Hsieh, and C. M. Wolfe, IEEE Electron Device Lett. **EDL-6**, 60 (1985).
[3] M. A. Ryan, M. W. Peterson, D. L. Williamson, J. S. Frey, G. E. Maciel, and B. A. Parkinson, J. Mater. Res. **2**, 528 (1987).
[4] G. A. Davis and C. M. Wolfe, J. Electrochem. Soc. **130**, 1408 (1983).
[5] G. A. Davis, M. W. Muller, and C. M. Wolfe, J. Cryst. Growth **69**, 141 (1984).
[6] G. A. Seryogin, S. A. Nikishin, H. Temkin, A. M. Mintairov, J. L. Merz, and M. Holtz, Appl. Phys. Lett. **74**, 2128 (1999).
[7] S. Francouer, G. A. Seryogin, S. A. Nikishin, and H. Temkin, Appl. Phys. Lett. **74**, 3678 (1999).
[8] B. Lita, R. S. Goldman, J. D. Phillips, and P. K. Bhattacharya, Appl. Phys. Lett. **74**, 2824 (1999).
[9] R. M. Feenstra, Phys. Rev. B **50**, 4561 (1994).
[10] N. A. Goryunova, M. L. Belle, L. B. Zlatkin, G. V. Loshakova, A. S. Poplavnoi, and V. A. Chaldysev, Sov. Phys. Semicond. **2**, 1126 (1969), and references therein.
[11] D. B. Gasson, P. J. Holmes, I. C. Jennings, B. R. Marathe, and J. E. Parrot, J. Phys. Chem. Solids **23**, 1291 (1962).
[12] A. A. Vaĭpolin and Yu. V. Rud', Sov. Phys. Solid State **29**, 364 (1987).
[13] J. M. Vandenberg, S. N. G. Chu, R. A. Hamm, M. B. Panish, and H. Temkin, Appl. Phys. Lett. **49**, 1302 (1986).
[14] R. S. Goldman, R. M. Feenstra, C. Silfvenius, B. Stålnacke, and G. Landgren, J. Vac. Sci. Technol. B **15**, 1027 (1997).
[15] O. Flebbe, H. Eisele, T. Kalka, F. Heinrichsdorff, A. Krost, D. Bimberg, and M. Dähne-Prietsch, J. Vac. Sci. Technol. B **17**, 1639 (1999).
[16] A. Y. Lew, C. H. Yan, C. W. Tu, and E. T. Yu, Appl. Phys. Lett. **67**, 932 (1995).
[17] Z. F. Zheng, M. B. Salmeron, and E. R. Weber, Appl. Phys. Lett. **64**, 1836 (1994).
[18] G. Lengel, R. Wilkins, G. Brown, M. Weimer, J. Gryko, and R. E. Allen, Phys. Rev. Lett. **72**, 836 (1994).
[19] A. Y. Cho, J. Appl. Phys. **46**, 1733 (1975).
[20] C. E. C. Wood and B. A. Joyce, J. Appl. Phys. **49**, 4854 (1978).
[21] M. Tao and J. W. Lyding, Appl. Phys. Lett. **74**, 2020 (1999).
[22] C. K. Shih, R. M. Feenstra, and P. Mårtensson, J. Vac. Sci. Technol. A **8**, 3379 (1990).